Marked Microspheres Assessment Using 1.5T Scanner for Embolization Follow up

H. JASSAR[1]

[1]Biomécanique et Génie Biomédical - Division Imagerie Médicale, Université de Technologie de Compiègne (UTC), Compiègne, France

Purpose:

Controlled embolization with MRI is an important innovation for fibroids and solid tumor treatment. Currently, angiography only allows the visualisation of flow inside the vessels, but particles used in the embolization procedure remain invisible and induced cm range errors. As a result, it is still a challenge to verify if these particles are located at the right places inside vessels. We used marked microspheres (*MR*MS*) with superparamagnetic iron oxide (*SPIO*), and the purpose of this works is to evaluate their visualization at 1.5 T with the help of *ex vivo* and *in vitro* models, and to predict the *in vivo* feasibility to detect *MR*MS* used as a vascular tumor emboli.

Methods:

1- Ex Vivo model: *2D T_2-w FSE-XL* (TR/TE = 3000/120 ms, ETL = 16, pixel size = 390×390 µm², and slice thickness = 2 mm) and *3D T_1-w SPGR* (TR/TE = 30/9 ms, flip angle = 45°, slice thickness = 1 mm, and pixel size = 390×390µm²) sequences were applied for the MR assessment of *MR*MS* and Embosphere microspheres (*EM*MS*) (Biosphere Medical, France) used as a control. 4 sizes of each kind of these microspheres (100-300, 300-500, 500-700, and 700-900 µm) were injected into 8 sheep kidneys. Their contrast with parenchyma and location in renal vasculature were assessed for each size. **2- First in Vitro model:** 4 sizes of *MR*MS* were embedded in hydrogel of a Petri dish, as a singlet, doublet, triplet, or cluster. *T_1-w* images were acquired *SPGR* sequence, MR and microscopic images were correlated in the function of microsphere distributions and sizes. **3- Second in vitro model:** (500-700µm) *MR*MS* range, which is preferred to achieve fibroid devascularisation [1], was embedded in a hydrogel of a Petri dish as different distributions, the feasibility of *in vivo* assessment was determined according to *in vivo* acquisition parameters, field of view (*FOV*), coil, and distance between coil and *MR*MS*. In addition, ultra Fast sequence (*3D Fiesta:* TR/TE = 7/3ms) was performed to minimize the motion artefact (respiratory) and increase signal-to-noise ratio (*S/N*).

Results:

Ex vivo (figure 1): MR*MS could be easily assessed with MRI. SPIO loading microspheres appear as black spots, whereas non loading microspheres remain invisible in *T_1-w* images. However, either *MR*MS* and *EM*MS* do not appear in *T_2 w* images (not shown here). Contrast measure between black spots and parenchyma shows an increased value as the microsphere size increased. The distance of black spots to the renal periphery decreased as the microsphere size increased. **First in vitro model (figure 2):** multiple microspheres appeared as a single black spot in *T_1-w* images as same as for a singlet microsphere. A strong linear correlation determined between the apparent and real sizes of MS ($R^2 = 0.8$) regardless their number. MRI magnification factor of single *MR*MS* diameters was 2.5 for all microsphere sizes. **Second in vitro model (figure 3):** The feasibility of *MR*MS* detection *in vivo* condition is determined according the using of different coils, FOV, and sequence.

Conclusion:

*MR*MS* can be detected with MRI to provide an accurate embolization of fibroids and solid tumors. Spatial resolution is optimized according to the magnification factor of *MR*MS* in MR images. *MR*MS* detection in *in vivo* conditions with ultra fast MR sequence is acceptable and will be useful in human application.

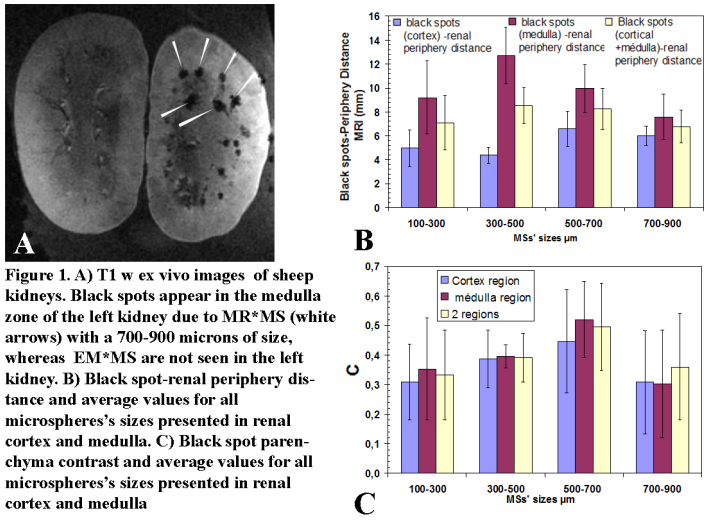

Figure 1. A) T1 w ex vivo images of sheep kidneys. Black spots appear in the medulla zone of the left kidney due to MR*MS (white arrows) with a 700-900 microns of size, whereas EM*MS are not seen in the left kidney. B) Black spot-renal periphery distance and average values for all microspheres's sizes presented in renal cortex and medulla. C) Black spot parenchyma contrast and average values for all microspheres's sizes presented in renal cortex and medulla

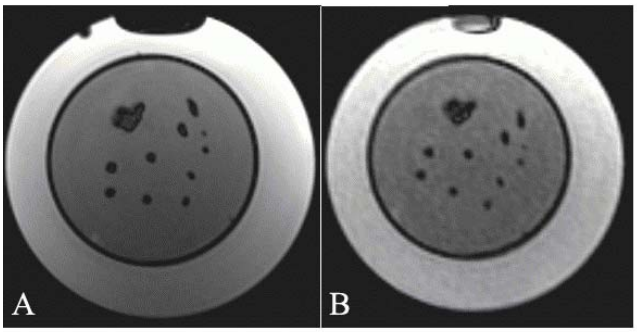

Figure 3. Ultra fast imaging of Petri dishes which contain MR*MS (500-700 microns) in: singlet, doublet, triplet and cluster configuration. A) MR image is obtained by Kneepa coil according to a 10 cm of Field of view and 31 sec of acquisition time. Kneepa coil is placed directly to the Petri dish. B) MR image is obtained by cardiac coil according to a 14 cm of Field of view and 31 sec of acquisition time. Cardiac coil is placed distantly from the Petri dish (8 cm)

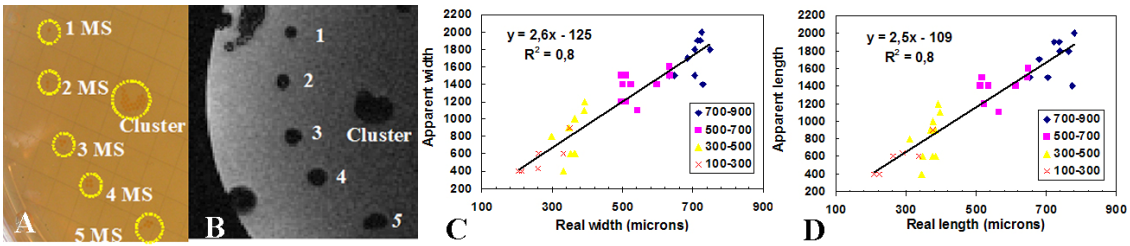

Figure 2. Microscopic and MR images of a quadrant of a Petri dish corresponding to a one size of MR*MS (500-700 microns). A) Microscopic image, a matrix of MR*MS grouped as a singlet, doublet, triplet and cluster (yellow round). B) T1 w image of a quadrant of the Petri dish. Black spots are in correspondence to different MR*MS configurations. C & D) The correlation between the apparent and real width and length of singlet MR*MS for all sizes

References:

[1] J. P. Pelage and al. J Vasc Interv Radiol 2003; 14:15–20